Numerical Simulation of the Rate of Dross Formation in Continuous Galvanizing Baths

Ajersch, Frank; Ilinca, Florin; Hétu, Jean-François; Goodwin, Frank E.

Proceedings of the Iron & Steel Technology Conference and Exposition (AISTech 2005), 2005-05-09

Numerical Simulation of the Rate of Dross Formation in Continuous Galvanizing Baths

Among the many challenges of the numerical simulation of the process of continuous galvanizing of steel sheet, the generation of dross particles is one of the most critical considerations. The presence of dross particles in different sections of a typical galvanizing bath is determined by both operational and configurational parameters that affect the nature of the flow, the temperature, and the distribution of the dissolved Al and Fe and of precipitated $Fe_3Zn_{24}Al_x$ (bottom dross) or $Fe_2Al_5Zn_x$ (top dross) particles. In order to quantify the effect of the flow field, temperature and concentration variations, the numerical simulation must take into account the physical and geometrical boundary conditions, the thermodynamics of the solution, as well as the industrially obtained data for iron dissolution from the strip, the rate of ingot melting and the rate of deposition of the coating.

Three-dimensional computer simulations have been carried out in a series of ILZRO-sponsored research projects and have been presented in several publications[1–3] for a typical bath configuration. Simulations were performed using the IMI in-house CFD software adapted for the solution of the heat and mass transfer, including the k-ε model of turbulence and buoyancy effects. The results of these simulations show the spatial distribution of temperature and composition of Fe and Al over a two-hour cycle with typical additions of ingots as required to maintain an overall heat and mass balance at the end of the two-hour period.

The present study compares the simulations of the standard configuration and operations with new operational and configurational parameters using a model for the entire bath volume, since the configurational parameters include asymmetric configurations. Other parameters that are considered are bath size, strip entry temperature, Al content of the ingot, gradual ingot immersion, as well as galvanize and galvanneal operations. The objective of this study is to carry out numerical simulations for flow, heat and mass transfer in order to determine the amount of dross particles generated within the liquid bath for a number of operational and geometric configurations as compared to a standard reference operating condition.

The rate of dross formation for 19 different conditions was calculated for a two-hour cycle. Differences in the evolution of the amount of dross formed in the galvanizing bath over this period were analyzed. The results can be used to provide guidelines for bath operation to minimize dross formation and accumulation.

Methodology

Figure 1 is a schematic of a typical modern galvanizing bath heated with two side inductors and with ingot melting at the center of the back wall of the bath. The basic bath configuration is given in Table 1, corresponding to a 250-ton bath and a deposition rate of 60 g/m^2 per side. It was previously established that ingot melting (complete immersion) takes 20 minutes and, at the deposition rate specified, an ingot is added at 60-minute intervals.[4] The inductors operate at maximum power during melting and at 20 percent of the maximum power during the period when no ingot is present, compensating for the heat loss from the bath. Under these conditions, an ingot containing 0.50 percent Al is added every hour, and the Fe and Al content at the end of

Authors

Frank Ajersch, professor, École Polytechnique de Montréal, Montréal, Que., Canada (frank.ajersch@polymtl.ca); **Florin Ilinca** and **Jean-François Hétu**, research officers, Industrial Materials Institute (IMI), National Research Council, Boucherville, Que., Canada (florin.ilinca@cnrc-nrc.gc.ca, jean-francois.hetu@cnrc-nrc.gc.ca); and **Frank E. Goodwin** (pictured), executive vice president, International Lead Zinc Research Organization (ILZRO), Research Triangle Park, N.C. (fgoodwin@ilzro.org)

insert Goodwin photo

Figure 1

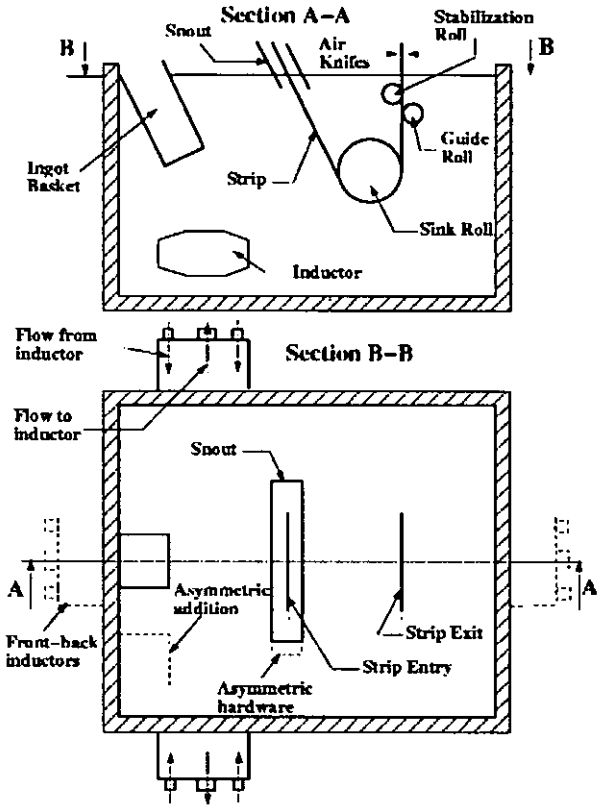

Schematic of the galvanizing bath.

the two cycles is almost identical to the starting conditions.

Boundary and initial conditions are imposed for the aluminum and iron concentrations. The initial aluminum and iron concentrations in the bath are considered 0.14 percent and 0.02782 percent in weight, respectively (the bath is considered saturated in Fe at the initial temperature). The limit of solubility is given by the following equation:[5]

Table 1

Parameters for the Base Configuration (250-ton Bath)

Parameter	Value
Strip entry angle (°)	27
Snout depth (inches)	8
Strip width (inches)	59
Roller depth (inches)	40
Bath height (inches)	96
Strip temperature (°C)	460
Strip velocity (m/second)	1.75
Deposition rate (g/m^2 per side)	60

$$\left(\frac{c_{Fe}}{100}\right)^2\left(\frac{c_{Al}}{100}\right)^5 = \exp\left(0.064 - \frac{36{,}133}{T+273}\right), \quad \text{for } c_{Al} \geq c^*_{Al} \qquad \text{(Eq. 1)}$$

$$(c_{Fe} - c^*_{Fe}) + 0.01(c_{Al} - c^*_{Al}) = 0, \quad \text{for } c_{Al} < c^*_{Al} \qquad \text{(Eq. 2)}$$

with

$$c^*_{Fe} = 0.023 + 1.5 \cdot 10^{-5}(T - 450)(T - 413.33) \qquad \text{(Eq. 3)}$$

$$\left(\frac{c^*_{Fe}}{100}\right)^2\left(\frac{c^*_{Al}}{100}\right)^5 = \exp\left(0.064 - \frac{36{,}133}{T+273}\right) \qquad \text{(Eq. 4)}$$

where c_{Fe}, c_{Al} are the weight concentrations of Fe and Al expressed in percentage (quantity in kg of Al or Fe for 100 kg of solution), and T is the temperature in °C. For values of the Al concentration larger than c^*_{Al}, the precipitates generated are in the form of Fe_2Al_5, and when the Al concentration is smaller than c^*_{Al}, then $Fe_3Zn_{24}Al$ precipitates are formed.

The configurational and operational conditions analyzed are given in Table 2.

The tasks involved for each simulation are as follows:

- Defining the geometrical configuration.
- Creating the finite element meshes (191,162 nodes and 1,106,928 elements for the reference configuration).
- Determination of boundary conditions and process parameters.
- Running the simulations.
- Analysis of the results.

Using these steps, calculations were carried out to determine the value of the temperature, Al and Fe content, as well as the precipitated amount of either Fe_2Al_5 or $Fe_3Zn_{24}Al$ for each of the 19 conditions. Values for specific regions at the front and back, as well as at different depths, were presented in the ILZRO report[6] and in other recent publications.[1–2,7] This study presents the average value of the bath temperature and the total amount of dross present at any instant over the two-hour period and determines the total amount of new dross generated for each of the cases.

Results

Bath Temperature — The variation of the average bath temperature over the two-hour cycle is shown in Figure 2 for a number of different conditions where differences in the temperature can be detected. The cases where ingots with different compositions are added or where the bath is unsaturated in Fe or Al were assumed to have no temperature effect. The dross is formed in small quantities, and the effect on the density of the Al content is small when compared with the buoyancy effect of the temperature. Snout position, asymmetric or different depth of immersed hardware had no significant effect on the overall mean temperature.

The overall heat balances for the six distinct heating cycles are shown in Figure 3. A lower strip temperature requires more heat after the melting period to maintain the bath temperature at the end of the cycle. Since the same size of induction heating was used for all simulated cases (two 450-kW inductors), it can be seen that the heat demand for the 500-ton pot (Figure 3d) is much larger than for the 100-ton pot (Figure 3c) to compensate for the heat losses at the bath surface and walls. Gradual immersion balances the heat loss with the induction heating, and thus no temperature increase is observed. Only a slight difference in heat demand was calculated for inductors placed at the front and back of the bath as compared to the standard location.

Effect of Al Content in the Ingot — The addition of 1-ton zinc ingots of 0, 0.5 and 1 percent Al to a saturated bath with 0.14 percent Al and 0.02782 percent Fe at 460°C were compared in order to illustrate the effect on the evolution of the total aluminum content in the bath, as well as the precipitated Al in the form of Fe_2Al_5. The results are shown in Figure 4a for the total Al content in the bath and in Figure 4b for the precipitated Al (as Fe_2Al_5). As would be expected for the same strip speed and deposition rate, the 0 percent ingot results in a decrease of the total Al content after two hours, and a 1 percent Al ingot results in an increase for the same period. Also, as expected, no new dross is formed for the 0 percent Al ingot, and increasing amounts of dross are found for the 0.5 percent Al ingot and the 1 percent Al ingot.

Effect of Al Content in the Bath — Three different bath compositions with total aluminum contents of 0.10, 0.14 and 0.20 percent Al at 460°C were compared during the addition of 0.5 percent Al ingots. The bath compositions are considered to be saturated in iron. The 0.20 percent Al bath was also computed for the oversaturated condition (0.06 percent Fe), which already contains an initial quantity of precipitated dross (258 kg of Fe_2Al_5) due to the excess value of Al and Fe over the saturated value of 0.14 percent Al and 0.02782 percent Fe.

The mean value of the total Al concentration is shown in Figure 5a. Assuming the Fe dissolution from the strip to be constant, the

Table 2

Simulated Configurations

1	Base configuration
2	Al concentration in ingot: 0 percent
3	Al concentration in ingot: 1 percent
4	Bath unsaturated with Fe
5	Bath with 0.1 percent Al and saturated with Fe
6	Bath with 0.2 percent Al and saturated with Fe
7	Bath with 0.2 percent Al and oversaturated with Fe (0.06 percent Fe)
8	Strip entry temperature 420°C
9	Strip deposition rate 100 g/m²
10	100-ton bath
11	500-ton bath
12	Side ingot charging
13	Gradual ingot charging at bath center
14	Gradual ingot charging at bath side
15	Front-back inductors
16	30-inch sink roll depth
17	Asymmetric hardware
18	Smaller snout size
19	Deeper snout

Figure 2

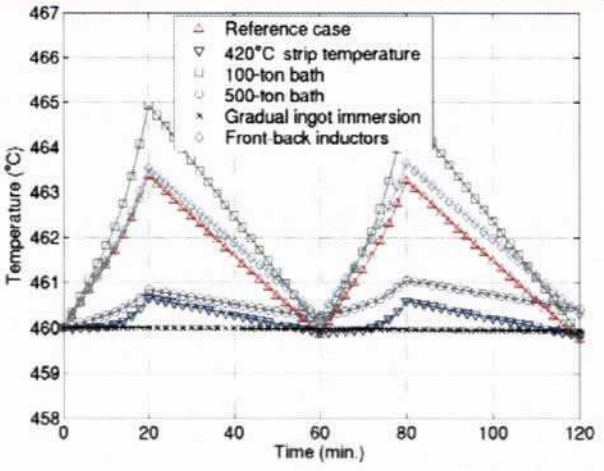

Mean temperature variation over the two-hour period.

Figure 3

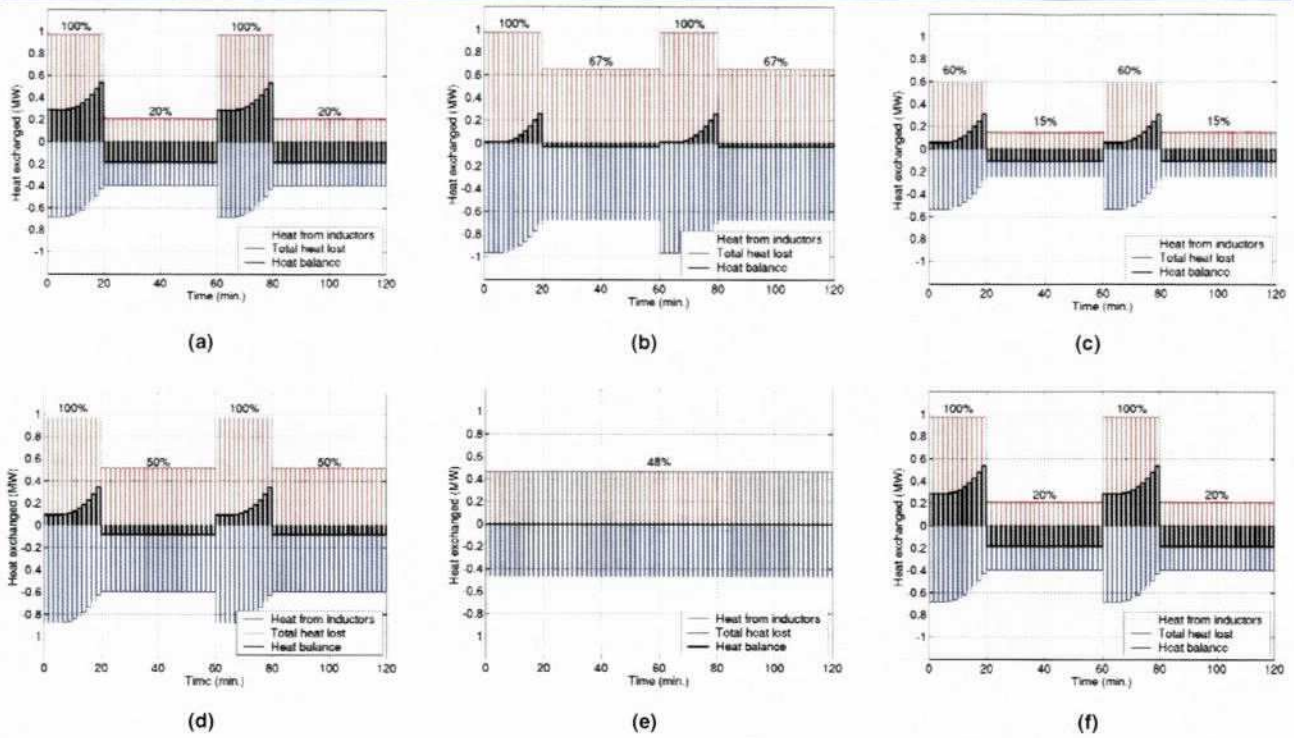

Total heat balance for different cases: (a) base configuration, (b) 420°C strip temperature, (c) 100-ton ingot, (d) 500-ton ingot, (e) gradual ingot immersion and (f) front-back inductor.

value of Al increases slightly during the ingot melting period, followed by a decrease due to the coating uptake on the strip. It should be noted that the variation of Al content for the 0.14 percent bath case is the same as shown in Figure 4a with a lower reference scale.

The precipitated dross as Fe_2Al_5 or $Fe_3Zn_{24}Al$ is shown in Figure 5b. It can be observed that the amount of new dross as Fe_2Al_5 is almost the same for the bath at 0.14 percent and for 0.2 percent Al, whereas the bath at 0.10 percent Al has a much smaller amount of precipitated Al. This is due to the precipitation of the δ phase $Fe_3Zn_{24}Al$, which contains much less Al. However, when the amount of precipitated Al is calculated in the

Figure 4

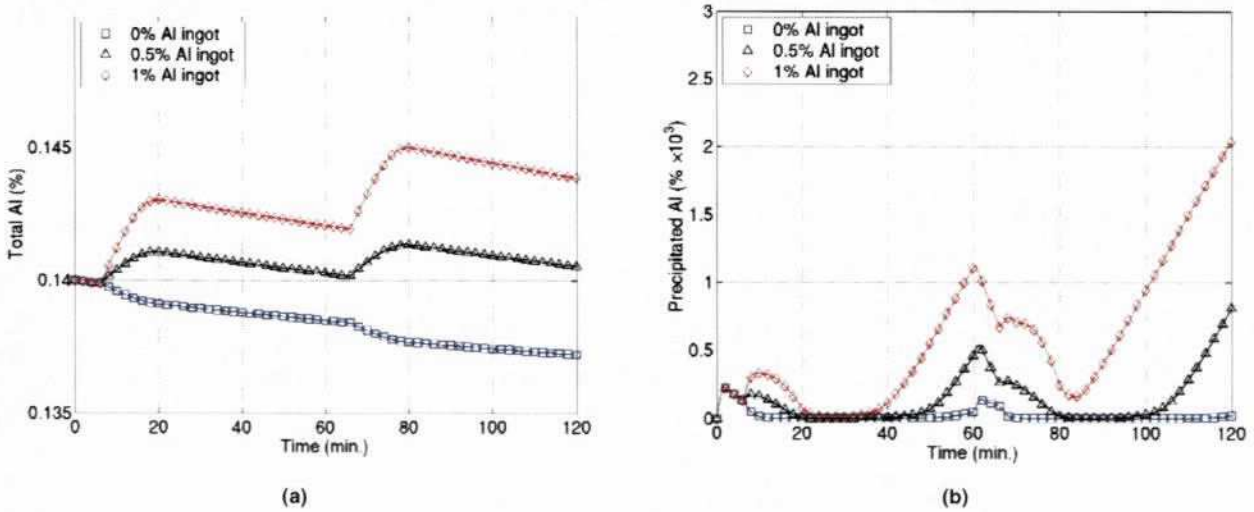

Effect of the Al content in the ingot on the total and precipitated Al in the bath: (a) total Al in the bath and (b) precipitated Al as Fe_2Al_5.

Figure 5

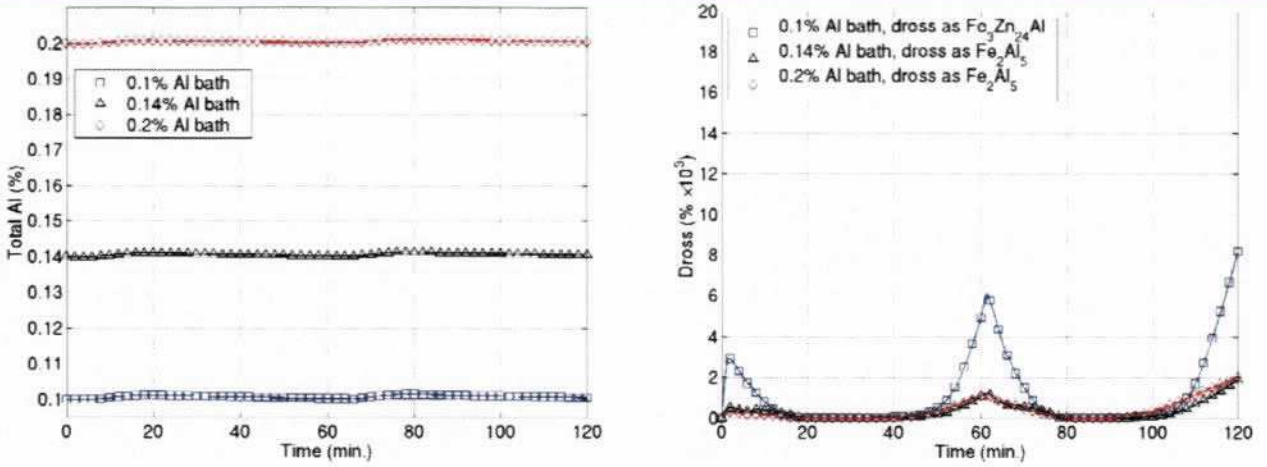

(a) (b)

Effect of the initial Al content in the bath on the total and precipitated Al in the bath: (a) total Al in the bath and (b) precipitated dross.

quantity of dross produced, the amount of dross formed at 0.10 percent Al (bottom dross) is much higher due to its composition ($Fe_3Zn_{24}Al$) where the top dross is Fe_2Al_5.

Effect of Strip Temperature — A lower strip temperature results in a smaller increase in the average bath temperature during the ingot melting period, as shown in Figure 2. The average temperature at the end of a cycle returns to the original temperature as a result of a heating cycle that uses a higher inductor capacity for the period after the ingot has melted in order to compensate for the additional heat required to heat the strip. Since the temperature of the strip attains 460°C within a very short interval of time, the total Al in the bath is the same as for the case of a strip temperature at 460°C, since the Al uptake on the coating is essentially the same as that shown in Figure 6a. The amount of precipitated Al as Fe_2Al_5 is the same at the end of the two-hour cycle; however, more dross is present in the bath during the two-hour period. For the standard case, dross is formed and then redissolved as the average bath goes through the temperature cycles.

Effect of the Coating Weight — Comparison is made between the standard case of 60 g/m² and a value of 100 g/m² using 0.50 percent Al ingot. Since more Al is taken up on the strip,

Figure 6

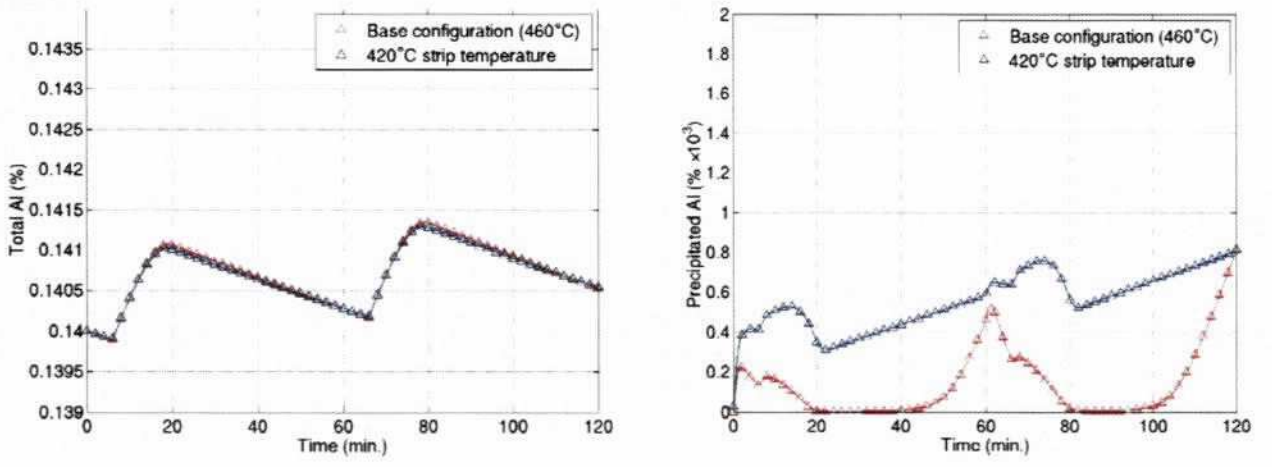

(a) (b)

Effect of the strip temperature on the total and precipitated Al in the bath: (a) total Al in the bath and (b) precipitated Al as Fe_2Al_5.

Figure 7

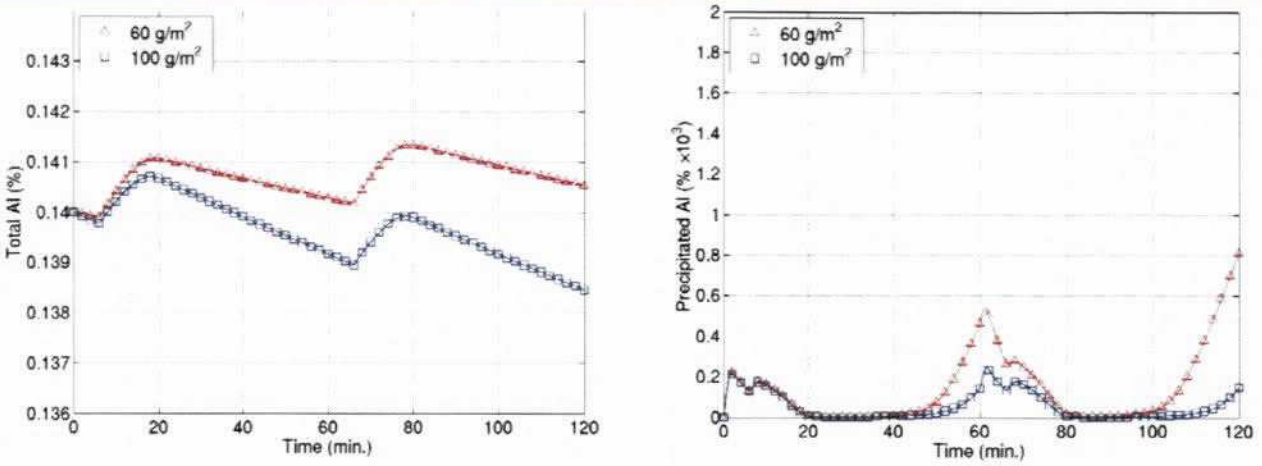

(a) (b)

Effect of the deposition rate on the total and precipitated Al in the bath: (a) total Al in the bath and (b) precipitated Al as Fe_2Al_5.

the amount remaining in the bath at the end of the two-hour cycle is lower than for the lower deposition rate. This is illustrated in Figure 7a, where the Al content in the bath decreases below the initial value as expected. It is assumed here that the average amount of Al in the coating is the same at 0.40 percent Al for both coating rates, although this may not be exactly the case in an actual operation. Since more Al is taken up by the strip for the higher coating rate, the precipitated Al as Fe_2Al_5 is lower at the end of the two-hour cycle, as shown in Figure 7b.

Effect of the Size of the Zinc Bath — Comparisons of zinc pot sizes were made with the 250-ton pot used as the base case. With the same ingot addition (0.50 percent Al) and the standard coating rate, the value of the total Al and precipitated Al were also calculated for a 100-ton and a 500-ton bath. As would be expected, the temperature increase is higher for the 100-ton pot, where the 20-minute melting period requires only 60 percent of the inductor capacity and the period between additions can maintain the end-of-cycle temperature at 460°C by operating at only 15 percent, as shown in Figure 3c. The total amount of Al in the bath increases much more sharply after the melting of the 1-ton ingot due to a smaller bath volume and the 60 g/m² deposition rate (Figure 8a). This is particularly evident in the second cycle shown in Figure 8b, when the precipitated amount of Fe_2Al_5

Figure 8

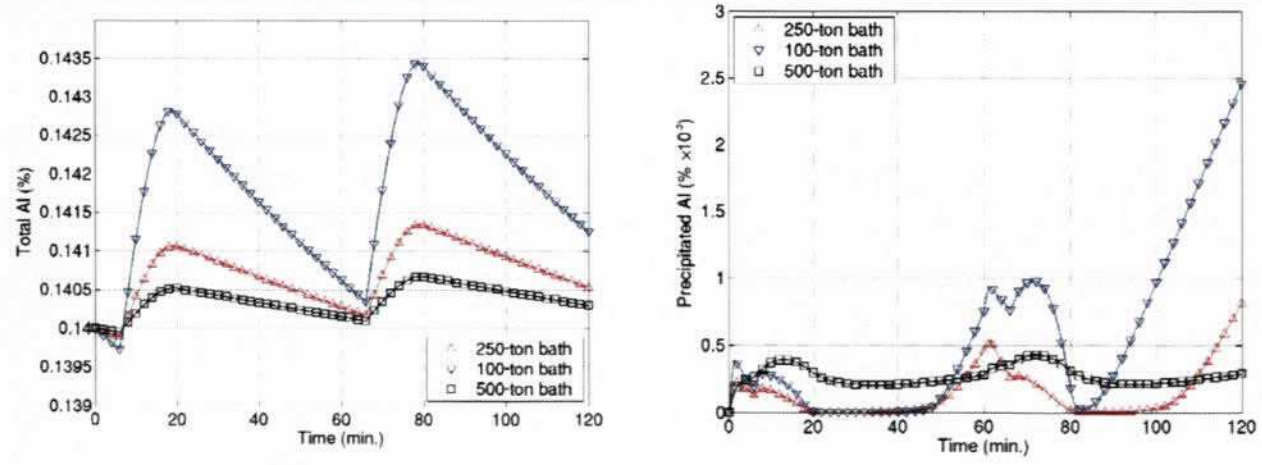

(a) (b)

Effect of the bath size on the total and precipitated Al in the bath: (a) total Al in the bath and (b) precipitated Al as Fe_2Al_5.

Figure 9

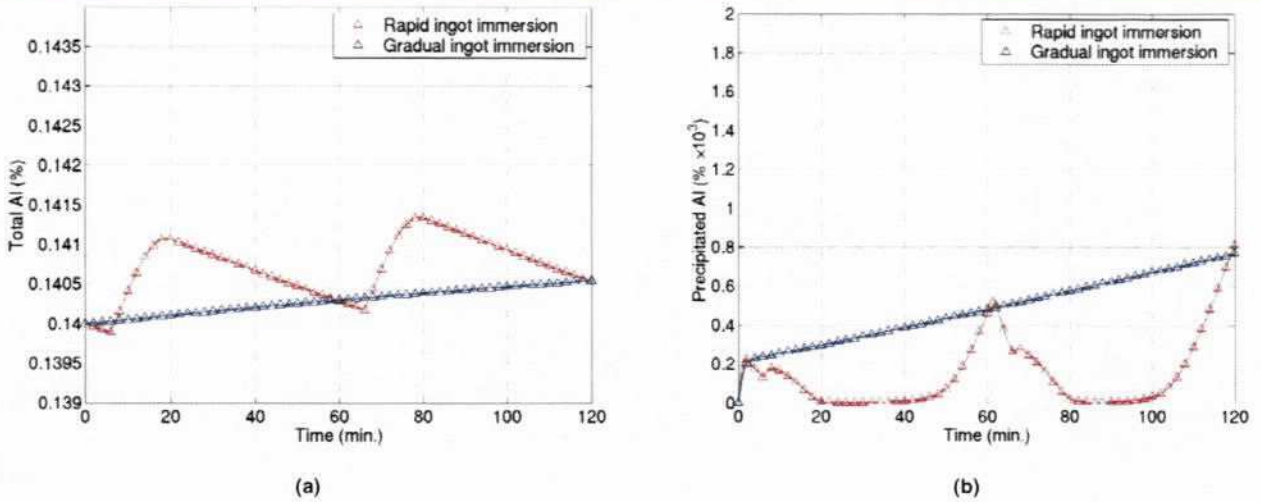

Effect of the gradual ingot immersion on the total and precipitated Al in the bath: (a) total Al in the bath and (b) precipitated Al as Fe_2Al_5.

increases sharply from the accumulation of Al in the bath.

Conditions for the larger bath show the opposite effect, in that the temperature rise during melting is smaller for the larger volume. The same inductors are at 100 percent capacity during the melting period and at 50 percent capacity during the nonmelting period in order to maintain the overall heat balance after two cycles. As a result of the larger volume, it would be expected to have a smaller increase in Al content in the bath, as shown in Figure 8a. As for the precipitated amount of Fe_2Al_5 particles shown in Figure 8b, the cyclic pattern is still present, but the maximum and minimum values are attenuated due to a much more constant temperature. At the end of the cycle, the precipitated content of Fe_2Al_5 is much lower (wt% of Fe_2Al_5). The total amount of new dross formed is also slightly lower than for the 250-ton bath.

Effect of the Ingot Immersion — Ingot immersion at the side of the back wall compared to the center location showed no difference in either the total Al or precipitated Fe_2Al_5, since the heat balance is identical. The only differences observed are the spatial distribution of Al in the bath. The values calculated at different specific locations are presented in the detailed analysis of the ILZRO report.[6]

Gradual ingot immersion balances the heat demand from ingot melting over the whole one-hour cycle. The inductor power was calculated to be 48 percent of the inductor capacity for the entire period. The temperature of the bath remains constant for the case of center or side ingot immersion, and the total Al content increases to the same value at the end of the two-hour period, as for the rapid immersion as shown in Figure 9a, without going through any cycles. Also, the precipitated amount of Fe_2Al_5 is the same at the end of the two-hour period with a constant gradual increase shown in Figure 9b.

Effect of Inductor Location — The mean bath temperature for the front and back inductor location is almost the same as for the side inductor location, as shown in Figure 3f. It is assumed that the total thermal input is the same for both cases for the melting and nonmelting periods. The small temperature difference is due to the slightly lower heat loss at the side walls and bath surface for the front-back inductor case. This results in a slightly higher temperature at the end of the two-hour period. The mean value of the total Al concentration (Figure 10a) is identical to the side inductor case, as would be expected from the identical ingot addition condition and deposition rate. The slight increase in the mean temperature of the bath for this configuration generated less precipitated Fe_2Al_5, as shown in Figure 10b.

Effect of Changes in Immersed Hardware Location — The influence of the sink roll depth, the asymmetric position of the roll assembly, snout depth and snout size have no effect on the total Al in the bath, nor on the precipitated amount for the two-hour cycle, when compared to the standard configuration, since the overall heat balance is the same. The flow patterns are different for each specific case and will result in different local variations of temperature and Al composition within the bath.

Figure 10

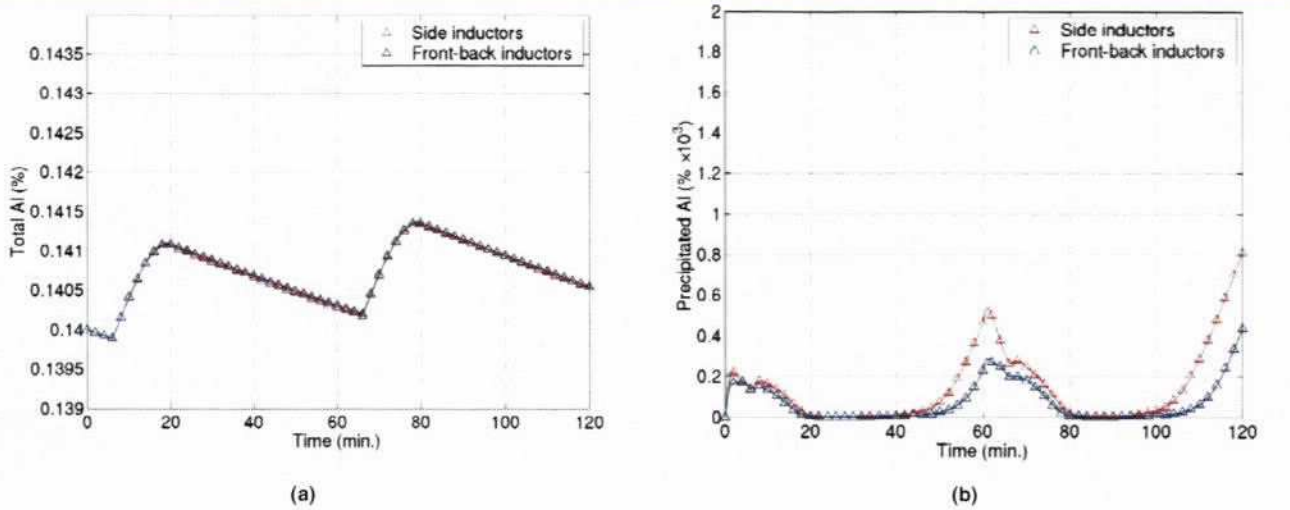

(a) (b)

Effect of the inductor position on the total and precipitated Al in the bath: (a) total Al in the bath and (b) precipitated Al as Fe_2Al_5.

Discussion

The coupled mass and heat transfer solutions have resulted in a clear and consistent representation of the distribution of aluminum in the bath for the simulated cycles of an ingot melting period followed by a period with no ingot in the bath. As the ingot melts, the total aluminum content increases or decreases according to the temperature- and motion-induced flows. The total aluminum represents the amount in solution and the amount that is in precipitated form. Assuming that the precipitated form of aluminum is Fe_2Al_5 and is very finely dispersed, it will be displaced at the same speed as the liquid zinc alloy in the bath. When these particles are transported into the region of higher temperature, they are assumed to dissolve instantly according to the solubility limits given by Tang.[5]

The series of solutions for the aluminum distribution is consistent with the rate of dissolution of an ingot and the uptake of aluminum from the bath. For a normal operation at 1.75 m/second strip speed and a coating weight of 60 g/m^2, the value of the aluminum content rises during the ingot melting stage and returns to a value only slightly higher than the initial value after a one-hour cycle. A higher mean Al concentration in the bath is reached when ingots with higher Al content are used, and inversely the Al concentration decreases when ingots with smaller Al content are melted. This confirms the need to vary the ingot composition for different coated products, taking into account strip width, strip speed and coating weight. Computations for the Fe concentration take into account the melting of ingots with no iron content and the dissolution of iron from the strip and into the bath. Because the rate of dissolution is greater than the rate of Fe uptake in the coating, the Fe concentration increases during the operation, part of which is found as precipitated Fe_2Al_5.

In analyzing the series of solutions of the total and precipitated aluminum in the bath calculated at the eight specific locations,[6] it can be observed that the amount of precipitated aluminum does not return to zero at the completion of the 60-minute cycle. Amounts of about 0.0006 percent Al above the solubility limit remain in the bath beyond this period and will tend to circulate throughout the bath. This could explain the formation of larger particles of Fe_2Al_5 due to nucleation and growth of these particles over time, according to a mechanism described generally as Ostwald ripening.

It is clearly shown that the heat input needs to be closely controlled during ingot melting to maintain a stable temperature of the bath. However, the inherent temperature gradients caused by ingot melting result in the precipitation of aluminum as Fe_2Al_5 in the cold regions of the bath.

The quantity of dross generated for each case after the two-hour period of simulation is presented in Figure 11. For the base configuration with an iron-saturated bath at 0.14 percent Al, the amount of new dross generated is 4.55 kg of Fe_2Al_5. With this reference point, the other configurational and operating conditions can be compared to this value, where the rate of iron dissolution from the strip is kept constant.

As should be expected, a 0 percent Al ingot will result in the lowest dross formation (0.13 kg), whereas the 1 percent Al ingot generates about 11.41 kg. Starting with a bath nonsaturated in iron also reduces the amount of dross formation. An iron-saturated bath with 0.1 percent Al generates a significant amount of

bottom dross ($Fe_3Zn_{24}Al$), whereas a bath saturated at 0.2 percent Al generates slightly less top dross than the reference condition. The case of the bath oversaturated in both Al and Fe (0.2 percent Al and 0.06 percent Fe) represents the values found for total Al and Fe in a typical operation. For the basic configuration, this represents a total Fe_2Al_5 dross content of about 258 kg in the bath. The additional dross formed for the basic coating rate is 5.22 kg after the two-hour period.

A larger bath (500 tons) generates slightly less dross than a smaller bath (100 tons), attributed to generally lower temperature gradients. Other variations — such as gradual ingot immersion, asymmetric hardware and variable snout dimensions — have only small effects on overall dross formation, but the locations of dross formation show some significant differences.

Figure 11

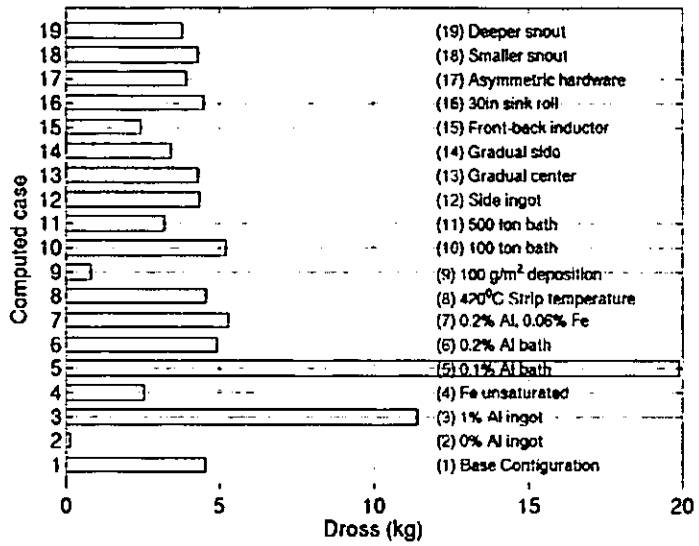

Dross formation for the different configurations.

Conclusions

Simulations have been carried out for 19 different operational and configurational parameters to determine the nature and amount of dross that is formed during typical operations of ingot addition. The use of ingots with higher Al content results in an increase in the mean Al concentration in the bath and the formation of additional dross. Gradual ingot immersion results in a very slow increase of dross and a smaller quantity of dross generated. The side ingot immersion determines the nonsymmetrical effect, especially near the ingot, and results in a smaller quantity of dross formed. The front-back inductor location resulted in a higher mean temperature in the bath, and consequently in a smaller quantity of dross. The asymmetry in hardware position has only small effects.

Specific locations of dross formation and accumulation depend on the local temperature variations in the bath due to heat input from the inductor and cooling of the bath near the melting ingot. For the period between ingot melting, the bath temperature is much more uniform and the dross becomes more evenly dispersed. A detailed numerical analysis of specific areas of the bath, such as the inner snout region or other critical areas, can clearly predict the tendency of dross formation at these locations.

Acknowledgments

The authors would like to acknowledge the International Lead Zinc Research Organization and the industrial sponsors for funding this project. The authors also wish to acknowledge the contribution of Michel Perrault in creating the bath mesh for the simulation.

References

1. Ajersch, F.; Ilinca, F.; and Hétu, J-F., "Simulation of Flow in a Continuous Galvanizing Bath: Part I, Thermal Effects of Ingot Addition," *Met. and Mat. Trans. B*, Vol. 35B, 2004, pp. 161–170.

2. Ajersch, F.; Ilinca, F.; and Hétu, J-F., "Simulation of Flow in a Continuous Galvanizing Bath: Part II, Transient Aluminum Distribution Resulting From Ingot Addition," *Met. and Mat. Trans. B*, Vol. 35B, 2004, pp. 171–178.

3. Ilinca, F.; Hétu, J-F.; and Ajersch, F., "Three-dimensional Numerical Simulation of Turbulent Flow and Heat Transfer in a Continuous Galvanizing Bath," *Num. Heat Transfer, Part A: Applications*, Vol. 44, 2003, pp. 463–482.

4. Toussaint, P.; Vernin, P.; Segers, L.; Winand, R.; and Dubois, M., "Experimental Study and Mathematical Modeling of Zinc Ingot Melting Behavior in Continuous Hot Dip Galvanizing Process," *Ironmaking and Steelmaking*, Vol. 22, No. 2, 1995, pp. 171–176.

5. Tang, N-Y., "Refined 450°C Isotherm of Zn-Fe-Al Phase Diagram," *Mat. Sc. Tech.*, Vol. 11, 1995, pp. 870–873.

6. Ajersch, F.; Ilinca, F.; and Perrault, M., "ZCO-8-8 Computer Aids for Galvanizing Bath Management — Further Development of the Galvanizing Bath Model," ILZRO report, March 2004.

7. Ajersch, F.; Ilinca, F.; Hétu, J-F.; and Goodwin, F.E., "Numerical Simulation of Flow, Temperature and Composition Variations in a Galvanizing Bath," *Canadian Metallurgical Quarterly*, to be published, 2005. ✦

This paper was presented at AISTech 2005 — The Iron & Steel Technology Conference and Exposition, Charlotte, N.C., and published in the AISTech 2005 Proceedings.